

Drivers of euphausiid species abundance and numerical abundance in the Atlantic Ocean

Tom B. Letessier · Martin J. Cox · Andrew S. Brierley

Received: 5 March 2009 / Accepted: 5 August 2009 / Published online: 2 September 2009
© Springer-Verlag 2009

Abstract Mid-ocean ridges are common features of the world's oceans but there is a lack of understanding as to how their presence affects overlying pelagic biota. The Mid-Atlantic Ridge (MAR) is a dominant feature of the Atlantic Ocean. Here, we examined data on euphausiid distribution and abundance arising from several international research programmes and from the continuous plankton recorder. We used a generalized additive model (GAM) framework to explore spatial patterns of variability in euphausiid distribution on, and at either side of, the MAR from 60°N to 55°S in conjunction with variability in a suite of biological, physical and environmental parameters. Euphausiid species abundance peaked in mid-latitudes and was significantly higher on the ridge than in adjacent waters, but the ridge did not influence numerical abundance significantly. Sea surface temperature (SST) was the most important single factor influencing both euphausiid numerical abundance and species abundance. Increases in sea surface height variance, a proxy for mixing, increased the numerical abundance of euphausiids. GAM predictions of variability in species abundance as a function of SST

and depth of the mixed layer were consistent with present theories, which suggest that pelagic niche availability is related to the thermal structure of the near surface water: more deeply-mixed water contained higher euphausiid biodiversity. In addition to exposing present distributional patterns, the GAM framework enables responses to potential future and past environmental variability including temperature change to be explored.

Introduction

The importance of euphausiids in marine ecosystems is reflected in a large volume of literature (Nicol 2003). They are mostly pelagic and are common in all the world's oceans. Euphausiids exert both top-down and bottom-up control on pelagic food webs (Verity et al. 2002) by grazing on primary producers and by acting as a food source for a suite of predators such as baleen whales, penguins, and commercially important species of fish. They are capable of large vertical migrations and contribute to the transport of bound carbon to the deep sea (Schnack-Schiel and Isla 2005; Tarling and Johnson 2006). Many studies have examined mesoscale to basin-scale drivers of euphausiid distribution (e.g. Trathan et al. 1993; Tarling et al. 1995; Gibbons 1997), but understanding the contribution of euphausiids to marine ecosystem processes globally, and the responses that the group may have to global change would be improved by further understanding of processes influential on ocean basin scales.

The pelagic realm is the Earth's largest habitat (Horn 1972). It overlays the continental shelves and the abyssal plains, which are interrupted by deep trenches, seamounts, volcanic islands and ridges. Amongst these bathymetric features of the plains, oceanic ridges have by far the largest

Communicated by U. Sommer.

Electronic supplementary material The online version of this article (doi:10.1007/s00227-009-1278-y) contains supplementary material, which is available to authorized users.

T. B. Letessier (✉) · M. J. Cox · A. S. Brierley
Pelagic Ecology Research Group, Scottish Oceans Institute,
University of St Andrews, St Andrews KY16 8LB, UK
e-mail: tbl@st-andrews.ac.uk

M. J. Cox
e-mail: mjc16@st-andrews.ac.uk

A. S. Brierley
e-mail: asb4@st-andrews.ac.uk

area and extend horizontally for more than 50,000 km in the Atlantic, Indian, Southern and Pacific Oceans combined (Kious and Tilling 1996). Ridges are underwater mountain chains rising several thousand metres from the seabed. They form at the junctions between tectonic plates. The tops of ridges usually have a valley running along their axes. Fracture zones punctuate ridges, running normal to the main ridge axis. Ridges may accommodate elevated benthic macrofaunal diversity compared to surrounding plains (Gebruk 2008) and are the sites of benthic and benthic-pelagic fisheries (Lorance et al. 2008). It is possible that ridges, as with seamounts (Dower et al. 1992), harbour elevated zooplankton populations. However, a lack of studies makes it difficult to draw many firm conclusions: ridges are often remote and hence inaccessible to traditional sampling methods due to rough terrain and have until quite recently been the focus of only a very low number of studies compared to similar depths and latitudes on the continental slopes and margins. Data on mid-ocean ridges are sparse.

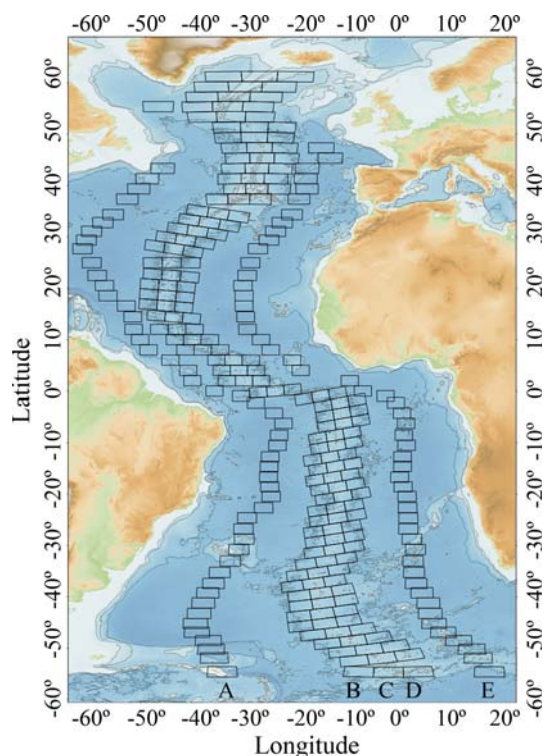


Fig. 1 Sampling cells ($n = 280$) on the Mid-Atlantic Ridge on a Latitude–Longitude projection (latitudes and longitudes plotted as if they were X and Y coordinates). Each cells is 370 km east to west and 222 km north to south, and is aligned with regionally-dominant fracture zones and faults. The three central columns (B , C and D) covered the MAR. Whenever distance from the ridge centre to the coastline enabled, columns A and E were halfway between the central cells and the coastline. The black lines demarcate the 1,000, 2,000 and 4,000 m isobaths. Figure was constructed using Geographical Information System Manifold[®] System 8.0

The Mid-Atlantic Ridge (MAR) extends from Iceland (64°N) in the north to the Southern Ocean (57°S; Fig. 1). Knowledge of the fauna of the MAR is presently limited largely to species that live directly on the MAR (e.g. benthic macrofauna, see Gebruk 2008), and pelagic nektonic species that live in proximity to the MAR (see Bergstad et al. 2008; Felley et al. 2008; Sutton et al. 2008). Studies investigating the drifting planktic animals living in the water column above the MAR are historically few, although a recent flurry of activity has begun to improve the picture (Stemmann et al. 2007; Gaard et al. 2008; Gislason et al. 2008; Heger et al. 2008; Hosia et al. 2008; Klimpel et al. 2008; Petursdottir 2008; Pierrot-Bults 2008; Sutton et al. 2008; Youngbluth et al. 2008). Yet it remains unclear whether planktic species are affected by the presence of ridges at all.

Even though the MAR has a major influence on the tidal regimes of the overlaying water column (Egbert and Ray 2001; Read et al. in prep) and on the gross circulation between the eastern and western basin of the north Atlantic (Harvey 1980), no biogeographical study has identified the MAR as a faunal barrier (Boltovskoy 1988; Gibbons 1997; Longhurst 1998; Beaugrand and Ibanez 2002; Beaugrand et al. 2002a). Furthermore, whilst seamounts have a number of potential effects on pelagic ecology, ranging, for example, from increased biodiversity/biomass to increased patchiness caused by predatory fish species intersecting vertically migrating zooplankton (Rogers 1994; Pitcher 2008), it is unclear to what extent these effects are replicated over ridges. Studies investigating deep acoustic scattering layers (Sigurdsson et al. 2002; Anderson et al. 2005; Sutton et al. 2008) have detected elevated pelagic biomass and diversity over the MAR as well as a modification of the physical structure of the benthic boundary layer (0–200 m above the sea floor). How this biomass is maintained without any apparent increase in surface production (Tilstone et al. 2009) is unknown. An investigation of the effect of the MAR on zooplankton would be beneficial both in terms of zooplankton ecology and because it could enable an assessment of the role of ocean ridges on biogeography.

In this study, we investigate the potential influence of a suite of environmental variables on the number of species and catch per unit effort (CPUE, a proxy for abundance) of euphausiids. A grid of cells spanning the majority of the latitudinal extent of the Atlantic Ocean was designed (Fig. 1), with particular focus on the MAR and its associated fracture zones. Each cell was populated with historical data on euphausiid species presence/absence and euphausiid CPUE when available, and with environmental data. A generalized additive model (GAM) approach (Wood 2006) was then taken to examine the influence of these environmental variables on euphausiid species abundance and CPUE.

Materials and methods

Grid cell design

The MAR runs broadly north to south but is intersected by fracture zones that result in numerous stepwise offsets along the ridge. A grid of cells was designed to cover the ridge and neighbouring open water. The grid comprised 280 cells (370 km east to west \times 222 km north to south, 5 columns by 59 rows Fig. 1). The east/west topography of the MAR determined the east/west extent of the cells, such that three cells spanned the width of the MAR: the central cell lay over the ridge crest and mid-axial valley, and the two adjacent cells covered the eastern and western MAR slopes. The north/south cell extent was set with consideration of the distance between the major fracture zones, such that multiple cells fitted entirely between fracture zones without any individual cells spanning them. Additional cells were positioned off ridge, midway between the ridge and the east and west coasts. These off-ridge cells served as latitudinally varying ‘controls’, being representative of non-ridge open ocean basin environment. All cells were populated, where possible, with euphausiid and environmental data (e.g. sea surface temperature, Fig. 2)

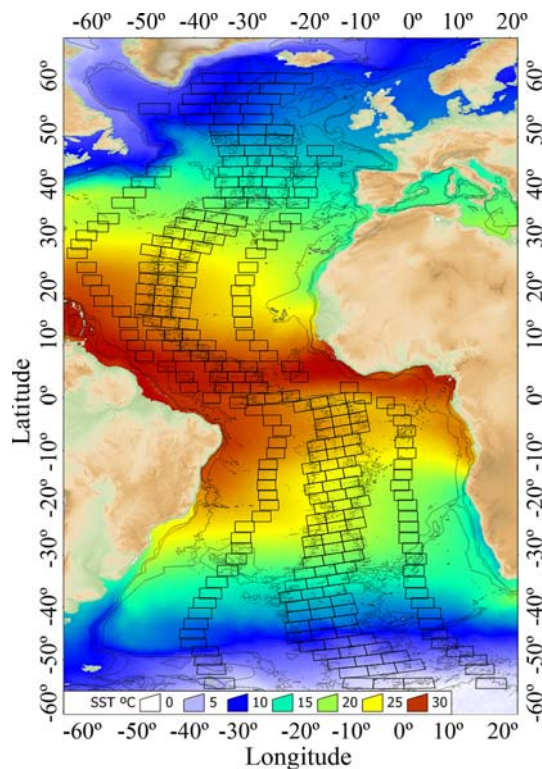


Fig. 2 Sea-surface temperature (°C) from SeaWiFS with grid cells overlaid. The 1,000, 2,000 and 4,000 m isobaths are shown. Figure was constructed using Geographical Information System Manifold® System 8.0

using the Geographical Information System Manifold® System 8.0 (CDA-International L 1993–2008).

Euphausiid numerical abundance and species abundance data sources

Species distributions and areas of occurrence

Data on Atlantic euphausiid species distribution ranges (Mauchline and Fisher 1969; Mauchline 1980; Brinton et al. 2000) were used to populate cells with species presence/absence data. Additional searches were conducted in the Global Biodiversity Information Facility for most up-to-date species distributions (updated to 2008), but the majority of records within that facility stem from well surveyed areas like coastal waters, and no species records were found there outside the ranges proposed by Brinton et al. (2000). Additionally, searches were conducted in the primary literature, including recent publications from research programmes that have sampled the MAR, for example, the UK Natural Environmental Research Council’s (NERC) Marine Productivity programme (e.g. Saunders et al. 2007b), The Census of Marine Life’s MAR-ECO: Patterns and processes of the ecosystem of the northern Mid-Atlantic (Wenneck et al. 2008) and NERC’s ECOMAR: Ecosystem of the Mid-Atlantic ridge at the sub-polar front and Charlie–Gibbs fracture zone (Read et al. in prep). These records were added to our database whenever they served to extend the older range of a species’ distribution. Together, all searches located a total of 54 species throughout the range of our sampling grid, with the species count per cell ranging from 5 to 30 (Fig. 3). The full data set can be accessed in supplementary spreadsheet 1 (cell labels are shown in supplement 2).

Continuous plankton recorder data

The continuous plankton recorder (CPR) has been deployed from ships of opportunity in the Atlantic (and North Sea) since 1931, taking underway samples from the top 10 m (Stevens et al. 2006). Euphausiids have been counted throughout that period, but have not routinely been identified to species level. The exception was in 1966–1967 when euphausiids were identified to species (Lindley 1977). CPR data from 1958 to 2006 ($n = 34,903$ samples falling within our grid of cells) were used to populate the cells with euphausiid numerical abundance. One CPR sample corresponds to a 10 nautical mile haul, along which $\sim 3 \text{ m}^3$ of water was filtered. Samples were available between 30°N and 63°N on the MAR (Fig. 4) but sampling effort was not distributed evenly. To account for the uneven spatial nature of CPR sampling (Fig. 4), euphausiid numerical abundance was scaled by effort (number of

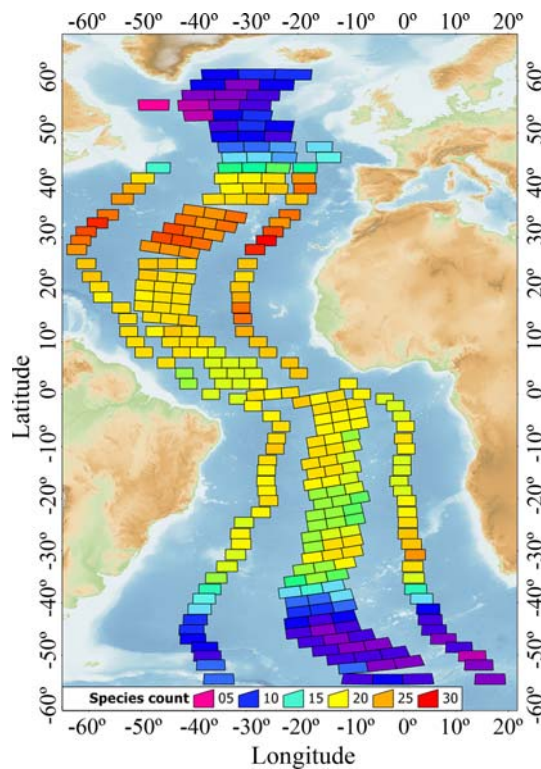


Fig. 3 Number of euphausiid species per cell (range 5–30). Figure was constructed using Geographical Information System Manifold® System 8.0

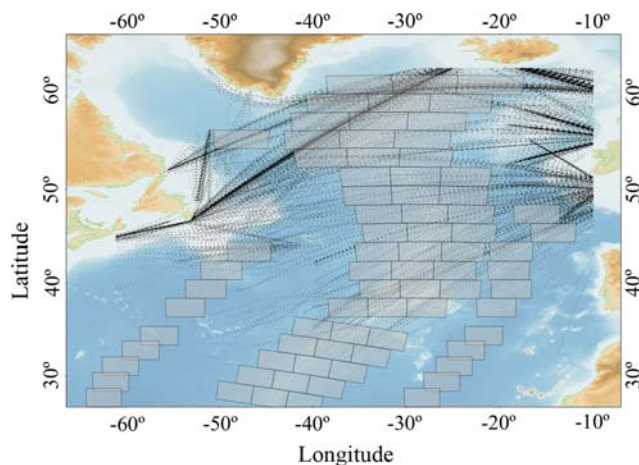


Fig. 4 Sampling cell grid and survey stations of the continuous plankton recorder in the north Atlantic ($n = 87,314$). Observations span from 1958 to 2006. Figure was constructed using Geographical Information System Manifold® System 8.0

hauls) to give catch per unit effort (CPUE, euphausiids per 3 m^3) in cell j where:

$$\text{CPUE}_j = \frac{1}{n} \sum_{i=1}^n \text{numerical_density}_i \quad (1)$$

The full data set can be accessed through supplementary spreadsheet 2.

Statistical modelling

A GAM approach was adopted to investigate the influence of various environmental variables on euphausiid species abundance and numerical abundance (Table 1). The GAM approach was chosen because it enabled both the identification of the statistically significant environmental characteristics (amongst the entire suite of candidate variables) and the scales of influence of the identified variables (magnitude of model parameter estimates) to be determined. Statistical analyses and GAM fitting were carried out using the R language (R Development Core team 2007). Separate models were fitted to predict species abundance and numerical abundance (from CPUE).

Explanatory variables

Candidate explanatory environmental variables were obtained from a variety of sources (see Table 1 for a list of the 51 variables and their abbreviations as used from hereon). Following Austin (2007), the candidate explanatory variables were split into two types: (1) proximal or direct variables, such as SST that may influence euphausiid species distribution directly (Gibbons 1997; Rutherford et al. 1999) and (2) distal or indirect variables, such as latitude that have no direct biological effect but are correlated with proximal variables and may be used as surrogates, for example, latitude is a surrogate for the number of daylight hours at a given location.

As proposed by Harrell et al. (1996), we followed the rule of thumb of limiting the degrees of freedom (q) of the explanatory variables offered for model selection to $q = m/10$, where m is the minimum number of observations in the response for each of the explanatory variables. Using this rule of thumb, the maximum degrees of freedom for explanatory variables entering the model selection procedure was $q = 28$ for the euphausiid species abundance and $q = 6$ for the euphausiid numerical abundances.

Of the 51 candidate explanatory variables, 20 were considered potential proximal and 31 distal environmental drivers (Table 1). Even for conventional linear modelling, where each explanatory variable ‘costs’ one parameter, our number of candidate variables exceeded the recommended number of degrees of freedom, m . Consequently, the number of candidate variables was initially reduced using the following rationale before the more formal model selection procedure was used.

1. Candidate explanatory variables that we considered to have no effect on euphausiid numerical abundance or species abundance were removed (i.e. Harrell 2001). For example, distance to the Conrad fracture zone,

Table 1 Explanatory variables used in our generalized additive model, and sources

Environmental variables	Abbreviation	Unit	Online source	Time range	Resolution/average over	Reference and rationale
Rossby radius of deformation	Rossby	km	Global Atlas of the first baroclinic Rossby radius: http://www.coas.oregonstate.edu/research/po/research/chelton/index.html	NA	1°/NA	Chelton et al. (2008) define Rossby radius as “the length scale of baroclinic variability longer than which internal vortex stretching is more important than relative vorticity”
Chlorophyll <i>a</i> concentration	Chl- <i>a</i>	mg m ⁻³	OceanColor: http://oceancolor.gsfc.nasa.gov/	2002–2008	1°/monthly	NASA ocean biology processing group (OPBG) moderate resolution imaging spectroradiometer (MODIS) - aqua monthly global 9-km products
Sea surface temperature	SST	°C	OceanColor: http://oceancolor.gsfc.nasa.gov/	2002–2008	1°/monthly	NASA OBPG MODIS-aqua Monthly global 9-km products
Dissolved and detrital organic matter absorption coefficient	Domac	m ⁻¹	OceanColor: http://oceancolor.gsfc.nasa.gov/	2002–2008	1°/monthly	NASA Garver–Siegel–Maritorena (GSM) SeaWiFS optical monthly global 9-km products
Particulate backscatter coefficient	Pac	m ⁻¹	OceanColor: http://oceancolor.gsfc.nasa.gov/	2002–2008	1°/monthly	NASA GSM SeaWiFS Optical Monthly Global 9-km Products
Salinity	Sal	ml l ⁻¹	OceanAtlas: http://odf.ucsd.edu/foa/	1990–1998	2°/NA	Osborne and Flinchem (1994)
Dissolved O ₂ concentration	O ₂	μmol l ⁻¹	OceanAtlas: http://odf.ucsd.edu/foa/	1990–1998	2°/NA	Osborne and Flinchem (1994)
Dissolved SiO ₃ concentration	SiO ₃	μmol l ⁻¹	OceanAtlas: http://odf.ucsd.edu/foa/	1990–1998	2°/NA	Osborne and Flinchem (1994)
Dissolved NO ₃ concentration	NO ₃	μmol l ⁻¹	OceanAtlas: http://odf.ucsd.edu/foa/	1990–1998	2°/NA	Osborne and Flinchem (1994)
Dissolved PO ₄ concentration	PO ₄	μmol l ⁻¹	OceanAtlas: http://odf.ucsd.edu/foa/	1990–1998	2°/NA	Osborne and Flinchem (1994)
Temperature at 50 m	T-50	°C	OceanAtlas: http://odf.ucsd.edu/foa/	1990–1998	2°/NA	Osborne and Flinchem (1994)
Temperature at 100 m	T-100	°C	OceanAtlas: http://odf.ucsd.edu/foa/	1990–1998	2°/NA	Osborne and Flinchem (1994)
Temperature at 150 m	T-150	°C	OceanAtlas: http://odf.ucsd.edu/foa/	1990–1998	2°/NA	Osborne and Flinchem (1994)
Sea level anomaly (height) mean	SSH-m	cm	AVISO: http://www.aviso.oceanobs.com/	2001–2008	0.33°/7 days	Ducet et al. (2000). The altimeter products were produced by Ssalto/Duacs and distributed by Aviso, with support from Ches. (Centre National d'Etudes Spatiales)
Sea level anomaly (height) variance	SSH-var	cm ²	AVISO: http://www.aviso.oceanobs.com/	2001–2008	0.33°/7 days	Ducet et al. (2000). Sea level variance was used as a proxy for water dynamics, which is known to be linked to zooplankton biomass heterogeneity (Piontkovski et al. 1995)
Mixed layer depth values for May and June	MLD-mj	m ³	US Naval Research Laboratory, Stennis Space Center: http://www7320.nrlssc.navy.mil/nmlid/nmlid.html	1900–1992	1°/NA	Kara et al. (2002). MLD is the depth to which where surface waters have been homogenized by turbulence. Values were cubed to reflect the volume of water affected
Mixed layer depth values for November and December	MLD-nd	m ³	US Naval Research Laboratory, Stennis Space Center: http://www7320.nrlssc.navy.mil/nmlid/nmlid.html	1900–1992	1°/NA	
Surface current velocity	SCV	m s ⁻¹	OSCAR: http://www.oscar.noaa.gov/	1992–2008	2°/5° (lon lat)/NA	Bonjean and Lagerhoed (2002). Values were missing in cell B1, B59, C1, C59, D1, D59, E59
Sea floor depth	Depth	m		NA	NA	
Distance to Mid-Atlantic Ridge	DR	km		NA	NA	The distance from each cell to the mid-axial valley (great circle distance, and distance along a degree of latitude)
Distance to fracture zones		km		NA	NA	The distance from each cell to predominant faults and fracture zones (<i>n</i> = 27)
Box coordinates		Decimal degrees		NA	NA	Latitude and longitude of the cell centre

Unless otherwise stated data resolution is a 1° latitude–longitude grid
 NA not applicable

Table 2 An example of the backwards model selection algorithm applied to the euphausiid species abundance generalized additive model

Model number	Model structure	GCV	Dropped term
1	Species abundance \sim longitude + Rossby + depth + Chl + s(SST, $k = 3$) + s(SiO ₃ , $k = 3$) + MLD-nd + MLD-mj + DR + SSH-var + factor (ridge side)	0.3059	Rossby
2	Species abundance \sim longitude + depth + Chl- a + s(SST, $k = 3$) + s(SiO ₃ , $k = 3$) + MLD-nd + MLD-mj + DR + SSH-var + factor (ridge side)	0.3038	SSH-var
3	Species abundance \sim longitude + depth + Chl- a + s(SST, $k = 3$) + s(SiO ₃ , $k = 3$) + MLD-nd + MLD-mj + DR + factor (ridge side)	0.3032	Factor (ridge side)
4	Species abundance \sim longitude + depth + Chl- a + s(SST, $k = 3$) + s(SiO ₃ , $k = 3$) + MLD-nd + MLD-mj + DR	0.3031	

A subset of the candidate models based on cross-validation scores (GCV) is given. Terms preceded by an “s” are smooths with “ k ” the dimension of the basis the smooth terms

located in the southern hemisphere, would probably not influence euphausiid numerical abundance in the northern hemisphere.

2. A correlation matrix between environmental variables was constructed and, following Wintle et al. (2005), one of each pair of explanatory variables with correlation $R > 0.7$ was discarded, keeping the variable that we deemed most likely to have a biologically founded impact. Since any potential influence of proximal explanatory variables could be interpreted directly, for example, $+1^\circ\text{C}$ increases euphausiid species abundance by x , whenever possible we retained proximal variables in preference to distal variables.

Following this process, 11 potential candidate explanatory variables remained for model selection (Table 2).

Functional form of environmental variables

We used a log-link function within our selected GAM framework to accommodate potential non-linear relationships between euphausiid response variables (either species abundance or numerical abundance) and explanatory variables (see Fox 2002 for a full list of assumptions). Incorporating smooth functions within the GAM framework enabled us to accommodate non-linear continuous explanatory variables (Wood 2006). Non-linear explanatory variable forms may have been quadratic, cubic or of a more complex shape. We had the option of allowing fully automated model selection i.e. allowing the model full freedom to select a non-linear form that balanced variance with complexity. However, Steyerberg et al. (2001) demonstrated that this approach may generate relationships that have no sensible biological grounding. Consequently, using the approach of Wintle et al. (2005), we inspected univariate GAMs visually, with five degrees of freedom (Austin and Meyers 1996), between each continuous candidate explanatory variable and the response variable. By restricting the models to five degrees of freedom, we

avoided generating relationships that were too biologically complex, yet permitted the models sufficient freedom to scope underlining biological patterns. Our knowledge of the biological processes and visual inspection of the resultant relationships was used to guide manual selection of the non-linear shape of candidate explanatory variable models (e.g. species diversity was set as a smooth function of sea surface temperature, as per Rutherford et al. (1999)). Where non-linear candidate explanatory forms were found to exist, it was the manually selected, non-linear forms that were used as candidate explanatory variables during final automated model selection.

Species abundance model selection

The bimodal nature of the euphausiid species abundance data (Fig. 5) required that the modelling framework should estimate the dispersion parameter (i.e. mean \neq variance). Therefore, we selected a quasi-Poisson error distribution (to estimate dispersion) and a log-link function (to account for the bimodal frequency distribution). The selection of a quasi-likelihood error distribution meant that, for the

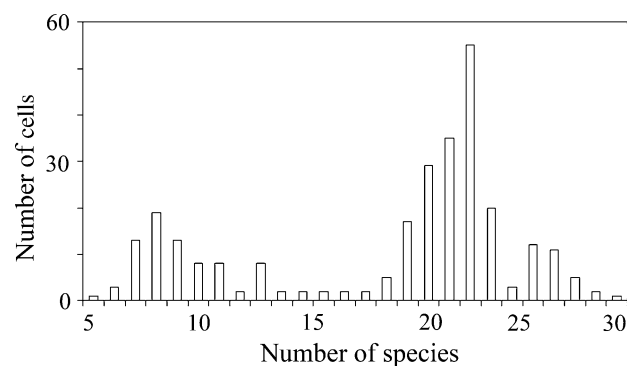


Fig. 5 Number of cells containing a given number of euphausiid species. The lowest species abundance was located at high latitude and the highest at mid-latitude in the northern hemisphere (see Fig. 4). Figure was constructed using Microsoft® Office Excel 2003

euphausiid species abundance investigation, model selection had to be carried out using the model generalized cross-validation score (GCV, Wood 2006). The GCV score was employed because more conventional likelihood-based model selection approaches, such as Akaike information criteria (AIC, Akaike 1973; Burnham and Anderson 2002) are not possible with quasi-distributions since likelihoods cannot be calculated. The GCV score can be thought of as scaled AIC, in that the model with the lowest GCV score offers the optimum combination of fit and parsimony. A GCV score-based backwards model selection algorithm (Table 2) was used because this generally performs better than AIC in the presence of collinear variables (Harrell, 2001), and also includes all possible explanatory variables in the first candidate model.

Numerical abundance model selection

Numerical abundances were modelled using CPR CPUE data as the response variable, and a log-link function with a Gamma error distribution since CPUE was a continuous variable. Following Burnham and Anderson (2002), we set up competing hypotheses for the biological drivers of numerical abundance, and based our model selection on a subset of the explanatory variables. Within these explanatory variable subsets backwards selection using the GCV score was carried out.

Model evaluation

We evaluated model performances based on three of the four metrics used by Potts and Elith (2006): (1) Pearson's correlation coefficient, r , was used as an indication of the relative agreement of the observed and predicted values. (2) Model calibration was assessed by linear regression between the predicted and observed values; the intercept of the linear regression c provided an indication of bias, and the gradient m (3) provided a comparison between the spreads of the data and model predictions. A perfectly calibrated model would have $c = m = 1$.

Explanatory variable practical influence

The biological, or practical, influence of statistically significant explanatory variables for the selected euphausiid species and numerical abundance models was investigated as follows. All explanatory variables were set to their mean observed value. Model predictions were then made for each explanatory variable in turn, with the value of the explanatory variable being investigated adjusted first to the 2.5% then the 97.5% quantile of the explanatory variable observed values. The percentage change was calculated by standardizing the change of the response variable between

the quantiles of each explanatory variable (species abundance and CPR CPUE) by the difference in the response variables from its respective 2.5 and 97.5% quantile. For the smooth functions (SST and SiO_3), we assumed that the change between the quantiles was linear.

Results

Spatial patterns of distribution and abundance

Species abundance

The species abundance was typically high in mid-latitude and tropical regions, and low in higher latitudes (Fig. 3). The highest species abundance per cell (30) was found in the mid-latitude in the northern hemisphere, in the eastern mid-ocean cell (29.4°N 26°S). A peak in abundance was located off the coast of south east Africa. The lowest species abundance (5) was located in the Labrador Sea (Fig. 3).

Numerical abundance

The general pattern of euphausiid numerical abundance was a southward decrease in abundance in the northern hemisphere. The highest abundance of euphausiids was located in the Labrador Sea. High abundance was located in the area immediately north of the Charlie–Gibbs fracture zone and in the cell south of Iceland on the Reykjanes ridge. Low abundances were recorded predominantly south of the North Atlantic Drift Current.

Statistical modelling

Our modelling objective was to determine the influences of environmental variability on species- and numerical abundance of euphausiids. Models for both performed well in this regard, with the species abundance and numerical abundance GAMs explaining 86.9 and 83.3% of the variability (R^2), respectively (Table 3).

Table 3 Model performance metrics for the assessment of the performance of the euphausiid numerical and species abundance models

Model performance metric	Numerical abundance	Species abundance
Correlation (r)	0.92	0.93
Calibration intercept (b)	0.49	2.47
Calibration slope (m)	0.88	0.87
R^2	0.83	0.87

Table 4 *p* values for explanatory variables retained in our GAM species count and numerical abundance models

Environmental variables	Numerical abundance model <i>p</i> value	Species abundance model <i>p</i> value
Longitude	NA	$5.71e^{-08}$
Depth	NA	0.035
Chl- <i>a</i>	NA	$5.41e^{-12}$
MLD-nd	NA	$8.93e^{-05}$
MLD-mj	NA	0.036
DR	NA	$1.57e^{-05}$
SST	$<2e^{-16}$	$<2e^{-16}$
SiO ₃	0.00324	$<2e^{-16}$
SSH-var	$4.19e^{-16}$	NA

Variables that were not selected in the final model are denoted by NA

Model selection

Species abundance model

The selected explanatory variables for the species abundance model were SST, SiO₃, Chl-*a*, Longitude, MLD-nd, MLD-mj, depth and DR (Tables 2, 4). The differences between the predicted species abundance values at the 2.5 and 97.5% quantiles showed that the greatest change in numerical abundance was caused by changes in SST, followed by changes in SiO₃ (Table 5). An increase in the numerical value of these explanatory variables lead to an increase in species abundance. These terms were both fitted as smooths (Fig. 6). Other important proximate variables were Chl-*a*, MLD and depth. Increase in depth and DR lead to a decrease in species abundance, although the impact of

Table 5 Euphausiid species abundance model parameter estimates and associated confidence intervals

Explanatory variable	Explanatory variable value at the 2.5% quantile	2.50% estimate	SE	Explanatory variable value at the 97.5% quantile	97.50% estimate	SE	Estimated change (<i>n</i> species)	Percentage change
SST	2.613	5.18	0.32	27.88	22.98	0.46	17.80	84.76
SiO ₃	1.05	20.32	0.45	14.74	35.56	1.96	15.23	72.52
Chl- <i>a</i>	0.043	23.13	0.37	0.55	16.81	0.63	-6.32	-30.09
Longitude	-57.20	23.27	0.53	3.76	19.56	0.35	-3.71	-17.66
MLD-nd	20,102	21.89	0.36	2,420,529	18.44	0.67	-3.44	-16.40
MLD-mj	12,608	21.90	0.36	2,063,857	18.92	0.58	-2.98	-14.19
Depth	-5540.40	20.24	0.58	-2312.80	22.45	0.61	2.21	10.53
DR	0.000	21.39	0.29	1761.95	21.39	0.29	-0.00051	-0.0024

The influence of each explanatory variable on euphausiids species abundance is shown by predictions made at the 2.5 and 97.5% quantiles of the explanatory variable data values on the scale of the response variable. During the prediction all other explanatory variables were fixed at their mean value. SE is the standard error of the prediction and estimated change is the number of species prediction, made at the 2.5% and the 97.5% explanatory variable quantile. See “[Explanatory variable practical influence](#)” for the calculation of estimated change and the percentage change

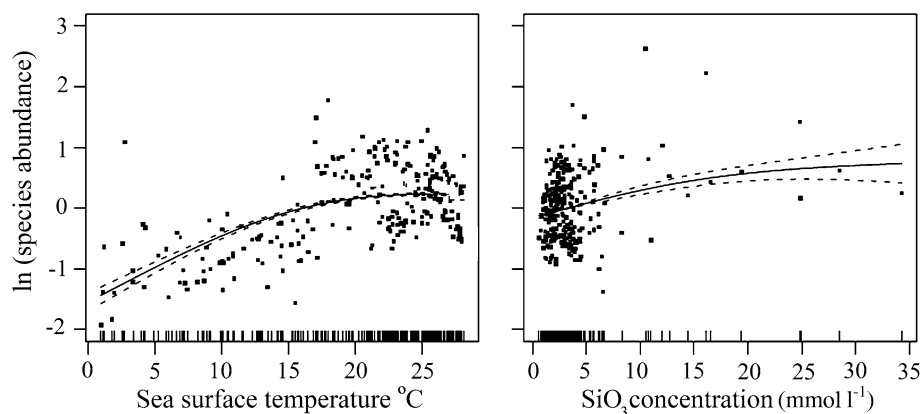


Fig. 6 Partial plots of the relationships between euphausiid species abundance and smooth terms of SST and SiO₃ concentration. The euphausiid species abundance counts on the y-axes are presented in the log domain, so that they can be interpreted in the same way as

linear regressions. The *dashed lines* represent the 95% confidence intervals for *curves*, and the *dots* are the residuals for the *curve* fit for a given explanatory variable. Figure was constructed using R v2.5.1 language

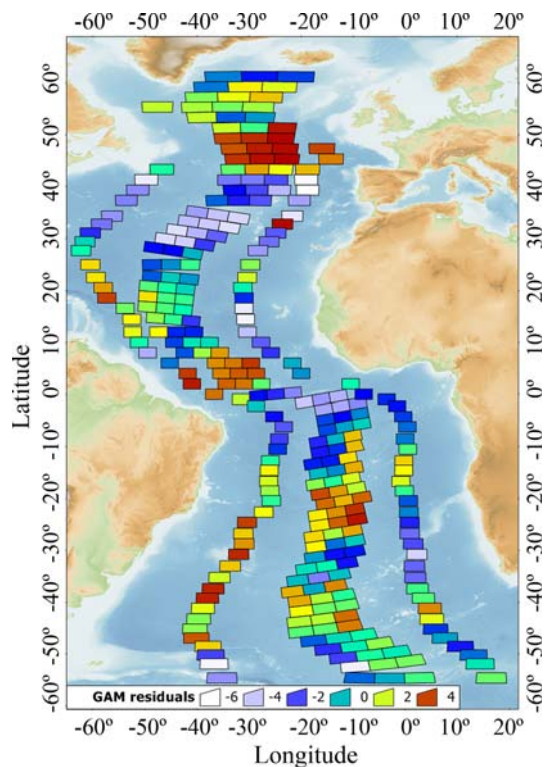


Fig. 7 Species abundance model residuals (observed minus predicted values). Figure was constructed using Geographical Information System Manifold® System 8

distance to the MAR was minor (percentage change credited to $DR < -0.003$). Longitude was the only distal variable selected, and it appeared that there was an eastward decrease in species abundance. The species abundance predictions were consistent with the general pattern of species abundance (Fig. 4) as demonstrated by the residuals plot (predicted minus observed values; Fig. 7). Areas of under-prediction occurred in the north (50°N , 30°W), the western tropics (5°N , 30°W) and the south-west (20°S , 15°W ; and 30°S , 30°W). Over-prediction occurred in the central north (30°N , 40°W) and eastern north Atlantic (40°N , 15°W), and along the western coast of South Africa.

Numerical abundance model

For the numerical abundance model, the use of the full suite of candidate variables was not possible because only six candidate degrees of freedom were available. Following Burnham and Anderson (2002), we set up competing hypotheses for the biological drivers of numerical abundance (“Functional form of environmental variables”) and eventually based our model selection on a subset of 6 of the 51 explanatory variables (see the first row of Table 2). Within these explanatory variable subsets, backwards selection using the GCV score was carried out. The selected

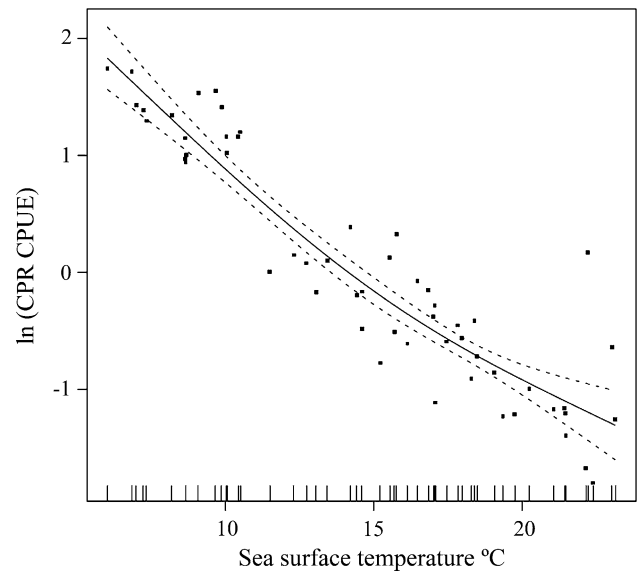


Fig. 8 Partial plot of the relationship between catch per unit effort (CPUE) of euphausiid numerical densities obtained from continuous plankton recorder (CPR) observations and smooth terms of SST. The fitted curve shows the relationship between SST and CPR CPUE. The dashed lines represent the 95% confidence intervals for the curve, and the dots are the residuals for the curve fit and the SST. SSTs are annual means per sampling cell between 2002 and 2008. Figure was constructed using R v2.5.1 language

explanatory variables were a non-parametric smooth of the relationship with SST, and linear relationships with SiO_3 and SSH-var (Fig. 8; Table 6). The difference in numerical abundance at the 2.5 and 97.5% quantiles indicated that increased SST and increased SiO_3 led to decreases in the numerical abundance of euphausiids (Table 6), whereas increased SSH-var led to increased numerical abundance of euphausiids. SST was the most important driver of variation in euphausiid numerical abundance.

Model performance

Under the model assessment criteria proposed by Potts and Elith (2006), both species count and numerical abundance models performed adequately, as demonstrated by the high correlation between predicted and observed values (Table 5). The calibrations revealed some evidence of bias in the model predictions, particularly for the numerical abundance model that had a low intercept parameter. There was some under dispersion in the species abundance data, as indicated by the high dispersion parameter (0.291), thus validating our choice of quasi-Poisson distribution.

Discussion

The aim of this investigation was to determine what factors, if any, influenced the distribution and abundance of

Table 6 Euphausiid numerical abundance model parameter estimates and associated confidence intervals

Explanatory variable	Explanatory variable value at the 2.5% quantile	2.5% estimate	SE	Explanatory variable value at the 97.5% quantile	97.5% estimate	SE	Estimated change (<i>n</i> euphausiids)	Percentage change
SST	6.91	14.77	1.82	22.774	0.8289	0.121	−13.94	−129.19
SSH-var	17.87	2.212	0.189	316.7	4.606	0.591	2.394	22.18
SiO ₃	2.100	3.58	0.521	6.914	1.737	0.232	−1.843	−17.08

The influence of each parameter on euphausiid numerical abundance is shown by predictions made at the 2.5 and 97.5% quantiles of the explanatory variable data values on the scale of the response variable. During the prediction all other explanatory variables were fixed at their mean value. SE is the standard error of the prediction, and estimated change in numerical abundance is the prediction made at the 2.5–97.5% explanatory variable quantile. See “[Explanatory variable practical influence](#)” for the calculation of estimated change and the percentage change

euphausiids in the Atlantic, giving special consideration to the MAR. Two ridge proxies, total depth and distance to ridge, were significant variables in the final species abundance model and thus provide evidence that the ridge itself has an influence on the species abundance of euphausiids. The numerical abundance of euphausiids was not influenced by these ridge proxies. Euphausiid species abundance was driven primarily by SST, and our results are consistent in this regard with present understanding of diversity patterns of euphausiids (Reid et al. 1978; Gibbons 1997) and other zooplankton groups (McGowan and Walker 1985).

Drivers of species abundance

Species diversity is traditionally believed to be highest in the tropics (Fuhrman et al. 2008). Several hypotheses, such as the species–energy hypothesis (Rohde 1992; Allen et al. 2002; Cardillo et al. 2005; Clarke and Gaston 2006), the species–area hypothesis (Currie et al. 2004), and the historical perturbation hypothesis (Stevens 2006) have been proposed to explain this latitudinal gradient. Our species abundance data showed, by contrast, that the greatest number of euphausiid species was located in the mid-latitudes, and not in the tropics. Moreover, our results indicate that the greatest change, some 84.75%, in euphausiid species abundance may be explained by variation in SST.

The exposure of Chl-*a* as a negative driver of euphausiid species abundance by our model is consistent with present understanding regarding the relationship between phytoplankton biomass and planktic diversity (Agard et al. 1996). Maximum micro-zooplanktic diversity levels have been found typically at intermediate levels of phytoplankton biomass (zooplanktic diversity is a bimodal function of phytoplankton biomass, see Irigoien et al. 2004); however, few studies have investigated the link between primary productivity and larger pelagic groups (but see Rosa et al. 2008).

Increases in the winter and summer averages for the volume of the mixed layer significantly decreased species abundance. The mixed layer depth is the depth to which

active turbulence has homogenized the water (Levitus 1982). Throughout our cell grid the highest species abundance values corresponded to intermediate levels of MLD depth (e.g. 100–150 m), as located at mid-latitudes (Floder and Sommer 1999). The link detected by our model is probably related to the influence of the MLD on primary productivity patterns: a basin scale and decadal study in the Pacific has shown that deepening of the MLD can increase primary productivity by up to 50% by supplying deeper waters with nutrients (Polovina et al. 1995) in subtropical waters. Furthermore, climate-driven deepening of the mixed layer is now driving down total production in the Pacific (Behrenfeld et al. 2006). As previously stated, Chl-*a* was significant in predicting decrease in species abundance. Here, we present evidence for a mechanism by which the depth of the mixed layer can affect patterns of pelagic species abundance, potentially through the intermediate of primary productivity.

A larger percentage of the increase in species abundance was driven by the increase in SiO₃ concentration. SiO₃ availability can limit phytoplankton growth in many systems (Hashioka and Yamanaka 2007). SiO₃ has an effect on the species abundance ratio of phytoplankton, and diatom growth rate is correlated with silicate concentrations (increases in SiO₃ may shift a flagellate dominated system to a diatom dominated system, see Escaravage and Prins 2002). Larger diatom species are often inaccessible to higher trophic level in planktic systems (such as some euphausiids) (see “[Drivers of numerical abundance](#)”), so silicate availability can influence community composition amongst primary grazers and beyond. Moreover, a high silicate concentration may inhibit competitive exclusion of certain mesozooplanktic species typical of high productivity regimes, thus increasing species abundance (Roy 2008).

Model residuals

There is some consistency and predictability in the species abundance model residuals. Under-prediction (positive residuals) occurs predominantly in the North Atlantic, and

is associated geographically with the sub-polar front. This discrepancy might be due to the mixing of different water masses (Iceland Current and North Atlantic Current) over the Charlie–Gibbs Fracture Zone (CGFZ). The CGFZ has been identified as a boundary between biomes (Longhurst 1998) and a faunal divide for zooplankton (Gaard et al. 2008), and is likely to harbour a mix of species arising from different water masses. Although this area is high in productivity, which should per our model decrease the number of species, we contend that the localized biogeographical properties of this region may counter the effect of high productivity.

Over-prediction (negative residuals) occurs near the east coast of Africa and along the fringe of the Benguela upwelling system. The cold, nutrient-rich upwelling water drives the high productivity of this area (Loncaric et al. 2007), and may serve to reduce the species abundance, as per our model results.

Over-prediction in the North Atlantic gyre might be linked to the formation of 18°C Mode Water (Goldthwait and Steinberg 2008) in the Sargasso Sea. Mode Water is characterized by uniform properties over an extensive depth range, and its formation in the Sargasso Sea is likely to have an impact on the MLD and may subsequently affect pelagic diversity (Michaels and Knap 1996).

Some over-prediction also occurs in the western sector of the Atlantic and may, in some cases, be linked to coastal plankton blooms associated with river runoff (Livingston 2007). River runoff enhances nutrient input and can stimulate enhanced primary productivity. Moreover, river runoff can, per Huston's dynamic equilibrium model, increase disturbance and subsequently reduce species diversity (see Huston 1979, highest species diversity is local in systems with intermediate disturbance) of a pelagic system through competitive exclusion (Agard et al. 1996). Under this scheme, disturbance is defined as rate of mortality of individuals caused by biotic or abiotic factors (Agard et al. 1996).

Our species abundance data have several limitations, the most potentially troublesome of which is the inconsistency of effort between cells. Species abundance by cell was compiled with reference to maps of species distributions, and these maps are themselves subject to sampling limitations: some regions of the Atlantic have been repeatedly sampled (such as the coastal regions of the British Isles), yet others have seldom been visited. Moreover, the sampling is further complicated by the use of different sampling gear and different sampling depths between trawls. This is potentially problematic as the vertical distribution of euphausiids varies on temporal basis (Endo and Wiebe 2007) and there is considerable temporal variation in euphausiid horizontal distribution on an annual (Saunders et al. 2007a) and monthly scale

(Trathan et al. 1993). It is likely that our estimates of species numbers in poorly surveyed areas, such as the central Mid-Atlantic, are low [certain sectors of the MAR have only been sampled once (see Gibbons 1997)]. This lack of effort could help explain the grouping of negative residuals in certain sectors of the tropical and south Atlantic. The most recent description of a previously unknown euphausiid species was in 1987 in the Pacific (Brinton 1987). We contend that euphausiid distribution is adequately known for our present purpose, and that for euphausiids generally the hypothetical species discovery curve is soon to reach the asymptote (Bebber et al. 2007). Thus, although our sampling might be biased, the broad conclusions we draw are probably not compromised by sampling effort limitations.

Drivers of numerical abundance

The most influential predictors of numerical abundance (in terms of % species change per interquantile range) were, in decreasing importance, SST, SSH-var and SiO_3 . The influence of SST on zooplankton abundance is well known, and instances of decreases in zooplankton abundance due to increases in SST have been recorded previously (McGowan et al. 2003; Wiafe et al. 2008). We estimated that the average effect of SST between the 2.5 and 97.5% quantiles to be -0.29 euphausiids $\text{m}^{-3} \text{ } ^\circ\text{C}^{-1}$.

Elevated zooplankton biomass is often found in frontal sectors and their areas of influence (Hense et al. 2003), where SSH-var is typically high. The effect of SSH-var that we observed on the numerical abundance may be due to increased productivity often associated with frontal features (Sambrotto et al. 2008, but also see Heath and Beare 2008): indeed the highest numerical abundance was located at the sub-polar front, an area that harbours high phytoplankton biomass (Tilstone et al. 2009). This observation validates the theory that copepod grazing on phytoplankton is reduced by predation from larger zooplankton (see Gaard et al. 2008). Our proxy for productivity (Chl-*a*), was not selected in the final numerical abundance model. This result is counter to the observation that zooplankton populations are bottom up limited (Edwards and Richardson 2004).

The influence of SiO_3 suggested by the model is consistent with present understanding of impacts of nutrient limitation on trophic interactions between primary productivity and primary consumers (see “Drivers of species abundance”). As previously stated, high SiO_3 is correlated with diatom growth rate. Moreover, a high diatom biomass can lead to a trophic mismatch, where the elevated phytoplankton biomass is inaccessible to higher levels (Escaravage and Prins 2002). We estimate the effect of SiO_3 to be -0.18 euphausiids $\text{m}^{-3} \mu\text{mol}^{-1} \text{ l}^{-1}$.

The large overall sample size ($n = 34,903$) and the broad seasonal span of the CPR data (sampling is conducted year round) means that our numerical abundance data are unlikely to be influenced by the high temporal frequency and mesoscale variability that is a feature of marine systems (Brierley et al. 2006; Sherwin et al. 2006). However, when inferring upon broad scale patterns of numerical abundance, the CPR data have many limitations. The CPR samples are geographically limited to a sector of the North Atlantic and the small size of the aperture (1.62 m^2) means that not all species are sampled equally (Kane 2009). Deeper living species will not be sampled at all due to the shallow depth (c. 10 m) of the tows. As a consequence, larger species may evade the net and abundance estimates for areas dominated by larger and deeper living species (such as *Meganycitphanes norvegica*) are likely to be low.

Effect of the Mid-Atlantic ridge

Our study has revealed a decrease in euphausiid species abundance with increasing ocean depth and distance from the MAR, although the change brought about by the latter was minor (-0.0024%). We suggest that the ridge serves to increase the number of species (the average depth of our central cell overlapping the ridge is 3,521 m as opposed to 4,806 m for our ocean basin cells). We contend that the mechanisms proposed by Rogers (i.e. predatory fish intercepting trapped zooplankton over raised bathymetry, 1994) and Pitcher (i.e. zooplankton enhancement, physical trapping of deeper scattering layers, 2008) are not sufficient to explain the influence of the MAR on the overlying zooplankton. However, at the present stage, we can only speculate as to what the mechanisms behind our observations are. We suggest that the increase in euphausiid species over the ridge is the result of the combined effect of biotic and abiotic factors. Biotic factors might include ontogenic horizontal and vertical migrations of euphausiids from neighbouring areas and greater depth horizons. Abiotic factors are less obvious, but we can theorize that the modification of surface currents by the ridge may lead to localized increases in species on and in the vicinity of the ridge. As per our results, this effect would diminish with increasing distance to the ridge. There is evidence of a modification of acoustic deep-sea scattering layers over the ridge (Sutton et al. 2008), which may be representative of increases in pelagic biomass and/or diversity.

We can theorize that a mean eastwards flow over a species-abundant ridge could lead to elevation of species in the eastern basin of the Atlantic compared to the west. Indeed, longitude did predict some of the patterns of euphausiid species abundance; however, it is unclear whether there is a biological reason for this.

In this study, we have detected an increase in the abundance of euphausiid species over the ridge. This result is not reflected by the numerical abundance model. Although it is unlikely that differences in ocean depth would be reflected in the numerical abundance of the top 10 m (depth sampled by the CPR) it is possible that an increase in available “substrate” (here represented by volume of water) could lead to a larger numerical abundance, and hence be reflected in the CPR data. As stated, our numerical abundance model did not detect the ridge as significant in predicting euphausiid abundance, leading us to one of three hypotheses:

- The CPR euphausiid data are inadequate for the detection of a ridge effect, as the effect of the ridge on euphausiids is not apparent in the numerical abundance in the top 10 m.
- The CPR euphausiid data are adequate for the detection of a ridge effect but need to be analysed to species level: numerical abundance are not affected by the ridge, but the species abundance are.
- The ridge does not affect numerical abundance of euphausiids.

With the data we have, we are unable to distinguish between hypotheses.

Conclusion and suggestions for further work

Our results suggest that the distribution and abundance of euphausiids is driven strongly by SST. The work is of ecological relevance as euphausiids are amongst the most important links in coastal and oceanic food webs and can be regarded as keystone sentinel taxa. Given the sensitivity of many additional predatory species to changes in euphausiid abundance (such as whales, see Konishi et al. 2008) there is an increasing need for understanding how abundance and distribution of euphausiids has and will change with ocean warming (Walther et al. 2002), and how euphausiids are affected by environmental variability. Large distributional changes in copepod assemblages have been reported due to increased SST (Beaugrand et al. 2002b), and similar processes could be relevant to euphausiid communities.

Through the use of our GAM framework, we detected an effect of distance from the ridge and of depth on the euphausiids. Since we used presence/absence data to compile the number of euphausiid species per cell, and not diversity indices (due to lack of numerical abundance coverage), our model is not as informative as it could be. We therefore contend that further sampling would increase rather than diminish our perception of the importance of the ridge. Further investigation is required to determine whether the responses we have observed relative to the MAR pertain to

ocean ridges generally. To that end, we are presently expanding our statistical modelling approach to euphausiids in the Pacific, in order to enable a comparison between ocean basins.

Acknowledgments We thank the Sir Alister Hardy Foundation for Ocean Science for the CPR data, and all the providers of environmental data used in our modelling. We thank the School of Biology at the University of St Andrews, and the United Kingdom Natural Environment Research Council, for funding, and C. Blight for help and expert advice with Geographical Information System software. The images and data used in this study were acquired using the GES-DISC Interactive Online Visualization ANd aNalysis Infrastructure (Giovanni) as part of the NASA's Goddard Earth Sciences (GES) Data and Information Services Center (DISC).

References

- Agard JBR, Hubbard RH, Griffith JK (1996) The relation between productivity, disturbance and the biodiversity of Caribbean phytoplankton: applicability of Huston's dynamic equilibrium model. *J Exp Mar Biol Ecol* 202:1–17
- Akaike H (1973) Information theory and an extension of the maximum likelihood. In: Petrov BN Cs'aki F (eds) Proceedings of the 2nd international symposium on information theory. Akademia Kaido, Budapest, pp 267–281
- Allen AP, Brown JH, Gillooly JF (2002) Global biodiversity, biochemical kinetics, and the energetic-equivalence rule. *Science* 297:1545–1548
- Anderson CIH, Brierley AS, Armstrong F (2005) Spatio-temporal variability in the distribution of epi- and meso-pelagic acoustic backscatter in the Irminger Sea, North Atlantic, with implications for predation on *Calanus finmarchicus*. *Mar Biol* 146:1177–1188
- Austin M (2007) Species distribution models and ecological theory: a critical assessment and some possible new approaches. *Ecol Model* 200:1–19
- Austin MP, Meyers JA (1996) Current approaches to modelling the environmental niche of eucalypts: implication for management of forest biodiversity. *For Ecol Manag* 85:95–106
- Beaugrand G, Ibanez F (2002) Spatial dependence of calanoid copepod diversity in the North Atlantic Ocean. *Mar Eco Prog Ser* 232:197–211
- Beaugrand G, Ibanez F, Lindley JA, Reid PC (2002a) Diversity of calanoid copepods in the North Atlantic and adjacent seas: species associations and biogeography. *Mar Eco Prog Ser* 232:179–195
- Beaugrand G, Reid PC, Ibanez F, Lindley JA, Edwards M (2002b) Reorganization of North Atlantic marine copepod biodiversity and climate. *Science* 296:1692–1694
- Bebber DP, Marriott FHC, Gaston KJ, Harris SA, Scotland RW (2007) Predicting unknown species numbers using discovery curves. *Proc R Soc Biol Sci* 274:1651–1658
- Behrenfeld MJ, O'Malley RT, Siegel DA, McClain CR, Sarmiento JL, Feldman GC, Milligan AJ, Falkowski PG, Letelier RM, Boss ES (2006) Climate-driven trends in contemporary ocean productivity. *Nature* 444:752–755
- Bergstad OA, Hoines AS, Orlov AM, Iwamoto T, Galbraith J, Byrkjedal I, Uiblein F (2008) Species composition and abundance patterns of grenadiers on the Mid-Atlantic Ridge between Iceland and the Azores. *Grenadiers world oceans: Biol Stock Assess Fish* 63:65–80
- Boltovskoy D (1988) Pelagic biodiversity: background, gaps and trends. In: Pierrot-Bults AC, Van der Spoel S (eds) Pelagic biogeography ICoPB II. proceedings of the 2nd international conference. IOC workshop report 142, pp 53–64
- Bonjean F, Lagerhoed GSE (2002) Diagnostic model and analysis of the surface currents in the tropical Pacific Ocean. *J Phys Oceanogr* 32:2930–2954
- Brierley AS, Saunders RA, Bone DG, Murphy EJ, Enderlein P, Conti SG, Demer DA (2006) Use of moored acoustic instruments to measure short-term variability in abundance of Antarctic krill. *Limnol Oceanogr* 4:18–29
- Brinton E (1987) A new abyssal euphausiid, *Thysanopoda minyops*, with comparisons of eye size, photophores, and associated structures among deep-living species. *J Crustac Biol* 7:636–666
- Brinton E, Ohman MD, Townsend AW, Knight MD, Bridgeman AL (2000) Euphausiids of the world ocean world biodiversity database CD-ROM Series
- Burnham KP, Anderson DR (2002) Model Selection and Multimodel Inference. Springer, New York
- Cardillo M, Orme CDL, Owens IPF (2005) Testing for latitudinal bias in diversification rates: An example using New World birds. *Ecology* 86:2278–2287
- CDA-International L (1993–2008) Manifold® system release version 8, Carson City
- Chelton BD, de Szoeke RA, Schlax MG (2008) Global atlas of first-baroclinic Rossby radius of deformation and gravity-wave phase speed. Oregon State University, Oregon
- Clarke A, Gaston KJ (2006) Climate, energy and diversity. *Proc R Soc Biol Sci* 273:2257–2266
- Currie DJ, Mittelbach GG, Cornell HV, Kaufman DM, Kerr JT, Oberdorff T, Guban JF (2004) A critical review of species-energy theory. *Ecol Lett* 7:1121–1134
- Dower J, Freeland H, Juniper K (1992) A strong biological response to oceanic flow part Cobb Seamount. *Deep-Sea Res Part I Oceanogr Res Pap* 39:1139–1145
- Ducet N, Le Traon PY, Reverdin G (2000) Global high-resolution mapping of ocean circulation from TOPEX/Poseidon and ERS-1 and-2. *J Geophys Res-Oceans* 105:19477–19498
- Edwards M, Richardson AJ (2004) Impact of climate change on marine pelagic phenology and trophic mismatch. *Nature* 430:881–884
- Egbert GD, Ray RD (2001) Estimates of M2 tidal energy dissipation from TOPEX/Poseidon altimeter data. *J Geophys Res* 106:22475–22502
- Endo Y, Wiebe PH (2007) Temporal changes in euphausiid distribution and abundance in North Atlantic cold-core rings in relation to the surrounding waters. *Deep-Sea Res Part I Oceanogr Res Pap* 54:181–202
- Escaravage V, Prins TC (2002) Silicate availability, vertical mixing and grazing control of phytoplankton blooms in mesocosms. *Hydrobiologia* 484:33–48
- Felley JD, Vecchione M, Wilson RR (2008) Small-scale distribution of deep-sea demersal nekton and other megafauna in the Charlie-Gibbs fracture zone of the Mid-Atlantic Ridge. *Deep-Sea Res Part II* 55:153–160
- Floder S, Sommer U (1999) Diversity in planktonic communities: an experimental test of the intermediate disturbance hypothesis. *Limnol Oceanogr* 44:1114–1119
- Fox J (2002) An R and S-plus companion to applied regression. Sage, London
- Fuhrman JA, Steele JA, Hewson I, Schwalbach MS, Brown MV, Green JL, Brown JH (2008) A latitudinal diversity gradient in planktonic marine bacteria. *Proc Natl Acad Sci USA* 105:7774–7778
- Gaard E, Gislason A, Falkenhaug T, Soiland H, Musaeva E, Vereshchaka A, Vinogradov G (2008) Horizontal and vertical

- copepod distribution and abundance on the Mid-Atlantic Ridge in June 2004. *Deep-Sea Res Part II* 55:59–71
- Gebruk AV (2008) Benthic fauna of the northern Mid-Atlantic Ridge: results of the MAR-ECO expedition. *Mar Biol Res* 4:1–2
- Gibbons MJ (1997) Pelagic biogeography of the south Atlantic Ocean. *Mar Biol* 129:757–768
- Gislason A, Gaard E, Debes H, Falkenhaus T (2008) Abundance, feeding and reproduction of *Calanus finmarchicus* in the Irminger Sea and on the northern Mid-Atlantic Ridge in June. *Deep-Sea Res Part II* 55:72–82
- Goldthwait SA, Steinberg DK (2008) Elevated biomass of mesozooplankton and enhanced fecal pellet flux in cyclonic and mode-water eddies in the Sargasso Sea. *Deep-Sea Res Part II* 55:1360–1377
- Harrell FE (2001) Regression modelling strategies: with application to linear models, logistic regression, and survival analysis. Springer, New York
- Harrell FE, Lee KL, Mark DB (1996) Multivariable prognostic models: issues in developing models, evaluating assumptions and adequacy, and measuring and reducing errors. *Stat Med* 15:361–387
- Harvey JG (1980) Deep and bottom water in the Charlie-Gibbs fracture zone. *J Mar Res* 38:173–182
- Hashioka T, Yamanaka Y (2007) Seasonal and regional variations of phytoplankton groups by top-down and bottom-up controls obtained by a 3D ecosystem model. *Ecol Model* 202:68–80
- Heath MR, Beare DJ (2008) New primary production in north-west European shelf seas, 1960–2003. *Mar Eco Prog Ser* 363:183–203
- Heger A, Ieno EN, King NJ, Morris KJ, Bagley PM, Priede IG (2008) Deep-sea pelagic bioluminescence over the Mid-Atlantic Ridge. *Deep-Sea Res Part II* 55:126–136
- Hense I, Timmermann R, Beckmann A, Bathmann UV (2003) Regional ecosystem dynamics in the ACC: simulations with a three-dimensional ocean-plankton model. *J Mar Syst* 42:31–51
- Horn MH (1972) Amount of space available for marine and freshwater fishes. *Fish Bull* 70:1295–1297
- Hosia A, Stemmann L, Youngbluth M (2008) Distribution of net-collected planktonic cnidarians along the northern Mid-Atlantic Ridge and their associations with the main water masses. *Deep-Sea Res Part II* 55:106–118
- Huston MA (1979) A general hypothesis of species diversity. *Am Nat* 113:81–101
- Irigoin X, Huisman J, Harris RP (2004) Global biodiversity patterns of marine phytoplankton and zooplankton. *Nature* 429:863–867
- Kane J (2009) A comparison of two zooplankton time series data collected in the Gulf of Maine. *J Plankton Res* 31:249–259
- Kara AB, Rochford PA, Hurlburt HE (2002) Naval Research Laboratory Mixed Layer Depth (NMLD) Climatologies. NRL Report 22
- Kious JW, Tilling RI (1996) Developing the theory: this dynamic earth. US Geological Survey, USA
- Klimpel S, Kellermanns E, Palm HW (2008) The role of pelagic swarm fish (Myctophidae: Teleostei) in the oceanic life cycle of *Anisakis* sibling species at the Mid-Atlantic Ridge, Central Atlantic. *Parasitol Res* 104:43–53
- Konishi M, Tamura T, Zenitani R, Bando T, Kato H, Walløe L (2008) Decline in energy storage in the Antarctic minke whale (*Balaenoptera bonaerensis*) in the Southern Ocean. *Polar Biol* 31:1509–1520
- Levitus S (1982) Climatological atlas of the World Ocean NOAA professional paper 13. US Government Printing Office, Washington DC, pp 173
- Lindley JA (1977) Continuous plankton records: The distribution of the Euphausiacea (Crustacea: Malacostraca) in the north Atlantic and the North Sea, 1966–1967. *J Biogeogr* 4:121–133
- Livingston RJ (2007) Phytoplankton bloom effects on a Gulf estuary: water quality changes and biological response. *Ecol Appl* 17:110–128
- Loncaric N, van Iperen J, Kroon D, Brummer GJA (2007) Seasonal export and sediment preservation of diatomaceous, foraminiferal and organic matter mass fluxes in a trophic gradient across the SE Atlantic. *Prog Oceanogr* 73:27–59
- Longhurst A (1998) Ecological geography of the sea. Academic Press, San Diego
- Lorance P, Large PA, Bergstad OA, Gordon JDM (2008) Grenadiers of the Northeast Atlantic—Distribution, biology, fisheries, and their impacts, and developments in stock assessment and management. *Grenadiers world oceans: Biol Stock Assess Fish* 63:365–397
- Mauchline J (1980) The biology of mysids and euphausiids. *Adv Mar Biol* 18:373–595
- Mauchline J, Fisher LR (1969) The biology of euphausiids. *Adv Mar Biol* 7:1–454
- McGowan JA, Walker PW (1985) Dominance and diversity maintenance in an Oceanic ecosystem. *Ecol Monogr* 55:103–118
- McGowan JA, Bograd SJ, Lynn RJ, Miller AJ (2003) The biological response to the 1977 regime shift in the California Current. *Deep-Sea Res Part II* 50:2567–2582
- Michaels AF, Knap AH (1996) Overview of the US JGOFS Bermuda Atlantic time-series study and the hydrostation S program. *Deep-Sea Res Part II* 43:157–198
- Nicol S (2003) Living krill, zooplankton and experimental investigations: a discourse on the role of krill and their experimental study in marine ecology. *Mar Freshw Behav Physiol* 36:191–205
- Osborne J, Flinchem EP (1994) Ocean Atlas NOAA/PMEL. Java Ocean Atlas, Seattle
- Petursdottir H (2008) Trophic interactions of the pelagic ecosystem over the Reykjanes Ridge as evaluated by fatty acid and stable isotope analyses. *Deep-Sea Res Part II* 55:83–93
- Pierrot-Bults AC (2008) A short note on the biogeographic patterns of the Chaetognatha fauna in the North Atlantic. *Deep-Sea Res Part II* 55:137–141
- Piontkovski SA, Williams R, Peterson W, Kosniriev VK (1995) Relationship between oceanic mesozooplankton and energy of eddy fields. *Mar Ecol Prog Ser* 128:35–41
- Pitcher TJ (2008) The sea ahead: challenges to marine biology from seafood sustainability. *Hydrobiol* 606:161–185
- Polovina JJ, Mitchum GT, Evans GT (1995) Decadal and basin-scale variation in mixed layer depth and the impact on biological production in the central and north Pacific 1960–88. *Deep-Sea Res Part I Oceanogr Res Pap* 42:1701–1716
- Potts JM, Elith J (2006) Comparing species abundance models. *Ecol Model* 199:153–163
- R Development Core Team (2007) R: a language and environment for statistical computing, reference index version 2.5.1. R Foundation for Statistical Computing, Vienna, Austria. ISBN 3-900051-07-0, <http://www.R-project.org>.
- Read J, Pollard RT, Miller P (In prep) Circulation across the Mid-Atlantic Ridge between 48 and 54°N during ECOMAR
- Reid JL, Brinton E, Fleminger A, Venrick EL, McGowan JA (1978) Ocean circulation and marine life. *Adv Oceanogr* 6:5–130
- Rogers AD (1994) The Biology of Seamounts. *Adv Mar Biol* 30:305–350
- Rohde K (1992) Latitudinal gradients in species diversity: the search for the primary cause. *Oikos* 65:514–527
- Rosa R, Dierssen HM, Gonzalez L, Seibel BA (2008) Large-scale diversity patterns of cephalopods in the Atlantic open ocean and deep sea. *Ecology* 89:3449–3461
- Roy S (2008) Spatial interaction among nontoxic phytoplankton, toxic phytoplankton, and zooplankton: emergence in space and time. *J Biol Phys* 34:459–474

- Rutherford S, D'Hondt S, Prell W (1999) Environmental controls on the geographic distribution of zooplankton diversity. *Nature* 400:749–753
- Sambrotto RN, Mordy C, Zeeman SI, Stabeno PJ, Macklin SA (2008) Physical forcing and nutrient conditions associated with patterns of Chl *a* and phytoplankton productivity in the southeastern Bering Sea during summer. *Deep-Sea Res Part II* 55:1745–1760
- Saunders RA, Brierley AS, Watkins JL, Reid K, Murphy EJ, Enderlein P, Bone DG (2007a) Intra-annual variability in the density of Antarctic krill (*Euphausia superba*) at south Georgia, 2002–2005: within-year variation provides a new framework for interpreting previous 'annual' estimates of krill density. *CCAMLR Sci* 14:27–41
- Saunders RA, Ingvarsdottir A, Rasmussen J, Hay SJ, Brierley AS (2007b) Regional variation in distribution pattern, population structure and growth rates of *Meganycitiphanes norvegica* and *Thysanoessa longicaudata* in the Irminger Sea, North Atlantic. *Prog Oceanogr* 72:313–342
- Schnack-Schiel SB, Isla E (2005) The role of zooplankton in the pelagic-benthic coupling of the Southern Ocean. *Scientia Marina* 69:39–55
- Sherwin TJ, Williams MO, Turrell WR, Hughes SL, Miller PI (2006) A description and analysis of mesoscale variability in the Faroe-Shetland Channel. *J Geophys Res* 111
- Sigurdsson T, Jonsson G, Palsson J (2002) Deep scattering layer over Reykjanes Ridge and in the Irminger Sea. *ICES CM*. M:09
- Stemmann L, Youngbluth M, Robert K, Hosia A, Picheral M, Paterson H, Ibanez F, Guidi L, Lombard F, Gorsky G (2007) Global zoogeography of fragile macrozooplankton in the upper 100–1000 m inferred from the underwater video profiler 4th International Zooplankton Production Symposium, Hiroshima, Japan, pp 433–442
- Stevens RD (2006) Historical processes enhance patterns of diversity along latitudinal gradients. *Proc R Soc Biol Sci* 273:2283–2289
- Stevens D, Richardson AJ, Reid PC (2006) Continuous plankton recorder database: evolution, current uses and future directions. *Mar Eco Prog Ser* 316:247–255
- Steyerberg EW, Eijkemans MJC, Harrell FE, Habbema JDF (2001) Prognostic modeling with logistic regression analysis: in search of a sensible strategy in small data sets. *Med Decis Making* 21:45–56
- Sutton TT, Porteiro FM, Heino M, Byrkjedal I, Langhelle G, Anderson CIH, Horne J, Soiland H, Falkenhaus T, Godo OR, Bergstad OA (2008) Vertical structure, biomass and topographic association of deep-pelagic fishes in relation to a mid-ocean ridge system. *Deep-Sea Res Part II* 55:161–184
- Tarling GA, Johnson ML (2006) Satiation gives krill that sinking feeling. *Curr Biol* 16:R83–R84
- Tarling GA, Ward P, Sheader M, Williams JA, Symon C (1995) Distribution patterns of macrozooplankton assemblages in the southwest Atlantic. *Mar Eco Prog Ser* 120:29–40
- Tilstone G, Smyth T, Poulton A, Huston R (2009) Measured and remotely sensed estimates of primary production in the Atlantic Ocean from 1998 to 2005. *Deep-Sea Res Part II*
- Trathan PN, Priddle J, Watkins JL, Miller DGM, Murray AWA (1993) Spatial variability of Antarctic krill in relation to mesoscale hydrography. *Mar Eco Prog Ser* 98:61–71
- Verity PG, Smetacek V, Smayda TJ (2002) Status, trends and the future of the marine pelagic ecosystem. *Environ Conserv* 29:207–237
- Walther GR, Post E, Convey P, Menzel A, Parmesan C, Beebee TJC, Fromentin JM, Hoegh-Guldberg O, Bairlein F (2002) Ecological responses to recent climate change. *Nature* 416:389–395
- Wenneck TL, Falkenhaus T, Bergstad OA (2008) Strategies, methods, and technologies adopted on the R.V. *G.O. Sars* MAR-ECO expedition to the Mid-Atlantic Ridge in 2004. *Deep-Sea Res Part II* 55:6–28
- Wiafe G, Yaqub HB, Mensah MA, Frid CLJ (2008) Impact of climate change on long-term zooplankton biomass in the upwelling region of the Gulf of Guinea. *ICES J Mar Sci* 65:318–324
- Wintle BA, Elith J, Potts JM (2005) Fauna habitat modelling and mapping: a review and case study in the lower hunter central coast region of NSW. *Austral Ecol* 30:719–738
- Wood S (2006) *Generalized additive models: an introduction with R*. Chapman and Hall/CRC, London
- Youngbluth M, Sornes T, Hosla A, Stemmann L (2008) Vertical distribution and relative abundance of gelatinous zooplankton, in situ observations near the Mid-Atlantic Ridge. *Deep-Sea Res Part II* 55:119–125